1997

A Self-consistent Power Relation for an Inverse Compton Scattering Theory

Robert A. Schill Jr.
University of Nevada, Las Vegas, robert.schill@unlv.edu

Laser and Particle Beams (1997), *vol.* 15, *no.* 3, *pp.* 367–378
Printed in the United States of America

A self-consistent power relation for an inverse Compton scattering theory

By ROBERT A. SCHILL, Jr.

Department of Electrical and Computer Engineering, University of Nevada at Las Vegas, 4505 Maryland Parkway, Box 454026, Las Vegas, Nevada 89154-4026, USA

(Received 23 June 1995; Accepted 14 April 1997)

In a self-consistent manner, the total power for linear inverse Compton scattering between a Gaussian electron beam colliding head on with a Gaussian laser beam is obtained. The theory is shown to agree with well-known limiting cases. Coupling among harmonic modes is explicitly shown in the resultant power relation. Even so, for the parameters of interest, harmonic modes are negligible compared to the fundamental mode. Total power calculations are of importance in detector calibration. The theory is applied using practical linear accelerator and laser parameters.

1. Introduction

One of the three main processes involved in the interaction of high-energy photons with atoms, nuclei, and electrons is Compton scattering (Longair 1992). When a photon interacts with a moving electron, the electron gains energy at the expense of the incident photon, yielding a lower energy scattered photon. A second Compton effect, which is just as important in the study of high-energy interactions, is inverse Compton scattering. Here, high-energy electrons scatter low-energy photons to a higher energy at the expense of the electrons' kinetic energy. This scattering process is of great importance in the study of high-energy astrophysics and free-electron sources.

Astrophysicists characterize the probability of scattering by means of cross sections (Tucker 1975; Longair 1992). The Thomson scattering cross section is used when quantum mechanical effects can be neglected. In this regime, $\gamma\hbar\omega_s \ll m_0c^2$, where m_0 and γ are, respectively, the electron rest mass and relativistic factor, and $\hbar\omega_s$ is the incident (source) photon energy. Outside this regime, quantum mechanical spin effects cannot be neglected, and the Klein–Nishina cross section is commonly used. From energy and momentum conservation considerations, the maximum energy a photon can acquire results from a head-on photon–electron collision, where the photon is backscattered along its original trajectory. The maximum scattered photon energy is $\omega \approx \gamma^2\omega_s$, assuming ultrarelativistic electrons. Astronomical observations indicate that radio and infrared photons are scattered into the ultraviolet and X-ray spectrums (Longair 1992). Further insights into the scattering process are obtained through a quantum mechanical formalism.

Numerous free-electron laser (FEL) studies have examined scattering from relativistic electron beams using a magnetostatic wiggler (Roberson & Sprangle 1989) or an electromagnetic standing wave (Tran *et al.* 1987). As the beam passes through these external fields, the electron beam undulates. Consequently, bremsstrahlung radiation results. The magnetostatic wiggler and the standing wave are effectively waves as far as the electron is concerned. Due to the periodic transverse acceleration, coherent radiation is produced. The inverse Compton mech-

 0263-0346/97 $11.00 + .10

anism and some FEL mechanisms are similar. In this paper, the generated radiation is not coherent. The Lienard–Wiechert potential method was used in the FEL with an electromagnetic standing wave pattern. The spontaneous emission or spectral energy distribution of a single electron is determined. Other means were used to calculate the powers generated from the beam.

Various authors (Vachaspati 1962; Brown & Kibble 1964; Sarachik & Schappert 1970; Bardsley *et al.* 1989; Mohideen *et al.* 1992) have theoretically and numerically examined the interaction of free electrons with an intense, focused, continuous, or pulsed laser beam. A classical theory (Sarachik & Schappert 1970) was developed for a single electron in an intense, elliptically polarized, plane electromagnetic wave. The radiated power, momentum, and harmonics were expressed in the laboratory and the rest mass frames. It is pointed out there that the linearly polarized wave cannot be described as a linear combination of the right and left circularly polarized waves because there would be no way of generating oscillatory motion transverse to the plane of polarization. This is due to the nonlinearity of the Lorentz force equation. Two recent papers numerically consider the classical motion of at most 100 electrons in a planar pulsed laser beam (Bardsley *et al.* 1989) and a Gaussian and a conical axicon focus pulsed laser beam (Mohideen *et al.* 1992). Bardsley *et al.* (1989) examine the relativistic dynamics of a single particle. The turn-on and turn-off properties of the laser pulse affect the electron's dynamic characteristics. To examine charge separation in a dense plasma, a simple model of space charge forces was incorporated in their numerical study. A harmonic restoring force in the direction of propagation of the laser was used. Phase-space portraits were presented. The second paper (Mohideen *et al.* 1992) provides a numerical simulation of the intensity of the radiated spectrum (normalized spectral electric field observed at a particular angle relative to the beam direction for different harmonic frequencies) of 1, 30, and 100 randomly distributed electrons interacting with a Gaussian and a conical axicon focus wave in the laboratory frame. The radiated frequency is a strong function of the observer's angular position. Consequently, it is not clear how to interpret their results on an experimental basis. The bandwidth resolution of a detector will be sensitive to this.

A recent set of studies on nonlinear Thomson scattering of intense laser pulses from beams and plasmas (Sprangle *et al.* 1989, 1992; Sprangle & Esarey 1992; Esarey *et al.* 1993; Ride *et al.* 1995) has been conducted by others. These authors developed a comprehensive study of linear and circular polarized laser fields incident on electrons of arbitrary energies. Space-charge effects are also included in the theory in a self-consistent manner. Even so, for their study on electron beams, this term is negligibly small and therefore is neglected in the development of the spectral intensity per solid angle. The authors state and emphasize in various places throughout the paper that nonlinear Thomson scattering can be used as a means to produce X rays (Sprangle *et al.* 1992; Esarey *et al.* 1993; Ride *et al.* 1995). Theoretical energy and wavelength comparisons have been made with conventional synchrotron sources containing magnetic wigglers or undulators (Kim 1989; Sprangle *et al.* 1992). Based on the constants of motion in conservation of canonical transverse momentum in one dimension and conservation of energy in the wave frame, the nonlinear electron motion is determined. They have shown that the backscattered radiation is a function of the intensity of the laser-beam intensity in the nonlinear regime. Even though this is an interesting result, stability of the backscattered radiation may be a concern for a practical device.

Independently, a classical linear theory is developed to examine the scattering of pulsed infrared and optical photon beams from a pulsed relativistic electron beam with the goal of developing a tunable VUV/X-ray source by means of inverse Compton scattering. The method of Lienard–Wiechert potentials (Jackson 1975) is used and the total power radiated by the beam is calculated analytically. It is well known that the scattered photon frequency is a function of the angular position of the observer. As a result, the concept of mode and the interpre-

tation of the spectral energy and spectral power distributions over a solid angle tend to lose physical meaning. That is, each term in the series characterizing the spectral quantities cannot be associated to a particular frequency or energy because the scattered frequency is a function of the observer's position. This point has been carefully considered in this theory. Therefore, using a verbiage consistent with other works, the term "harmonic" is used in a loose sense. In the limit when the dimensionless laser strength parameter $a_0 \ll 1$, the nonlinear theory developed by others (Esarey *et al.* 1993) agrees with the results obtained. It is shown in a power calculation that the backscattered radiation at the fundamental is many orders of magnitude stronger than at the harmonics. In the limit of a linear theory, only the first harmonic number contributes to the backscattered radiation along the axis. In synchrotron radiation theory, for a linearly polarized undulator, the amplitude of the odd harmonics is nonzero in the backscattered direction along the beam axis. These nonzero odd harmonics are due to second-order (nonlinear) effects arising from the laser beam's magnetic field interacting with the perturbed transverse motion of the electron beam. This results in a perturbation to the beam's drift velocity. When designing a calibration source, it is desired that the strength of the dominant frequency of operation be orders of magnitude greater than its harmonics. As a result, nonlinear effects in the backscattered direction are not desired. Realistic linear accelerator and high-energy CO_2 and ruby laser parameters are used. The Gaussian nature of the electron beam and the laser beam is incorporated in the theory in a consistent manner. The power radiated is not in general optimized when the waist of the electron beam equals the waist of the laser beam. Radiation reaction, space charge, and nonlinear effects have been neglected. The latter two approximations are consistent with the discussions developed in others' work (Esarey *et al.* 1993). One of the objectives of this study is to demonstrate that the scattered powers generated from a single pulse interaction for a narrow band of X-ray energies is large enough to be detected by a sensitive X-ray detector. The sensitivity of some of these detectors (e.g., the CsI windowless detector) is measured in terms of power over a bandwidth of operation. The total power over the region of the detector surface is the measurable parameter. Therefore, our concern is not with the brightness and flux parameters commonly used by the synchrotron community (Kim 1989) as it is with the angular power, the power within specified bandwidths, and the total power. A consistent theory is developed to yield the power directly from the intensity calculation without the need to resort back to the electron orbit, as required in power calculations using the relativistic Larmor formula (Esarey *et al.* 1993). It is shown that 10 mW of power up to better than tens of watts of power can be generated in respectable bandwidths from a 20- to 30-MeV linear accelerator. The backscattered photon energies are 712 eV (using a CO_2 laser and a 20-MeV electron source) or 24.5 KeV (using a ruby laser and a 30-MeV electron source). A source with such a property can be used for pulse mode calibration in the VUV and X-ray spectrum. The theory has been used in the study of a linear accelerator used as a VUV/X-ray source using the inverse Compton-scattering mechanism (Schill & McCrea 1997). Comparisons were made with large synchrotron sources used to generate similar radiation. Various applications were also examined. In the limit when the electron beam drift velocity approaches zero, the expected radiation pattern of a Hertzian dipole is demonstrated for a linearly polarized source wave. Consistency is established with energy and momentum considerations commonly used in quantum mechanical arguments. Retaining dominant terms, it is also demonstrated that the power series yields the same power radiated as obtained from a relativistic Larmor formula, assuming a Gaussian laser pulse passing through a uniform distribution of electrons.

An expression for the total power is formulated in a self-consistent manner in Section 2. The theory is compared to other existing theories in Section 3. The paper is concluded with an application and discussion in Section 4.

2. Expression for total power in a self-consistent formulation

A relativistic electron with z-directed velocity, $v_0\hat{z}$, charge q and rest mass m_0 interacts with an x-polarized, pulsed, monochromatic electromagnetic field (laser or photon beam) with angular frequency ω_s, and wavenumber k_s (figure 1). The profile of the beam perpendicular to the direction of propagation is Gaussian. The laser beam is focused in the interaction region. Let the beam be focused to its waist at $z = 0$. The beam waist is W_0. At and near the waist of the laser beam, the electric field is approximated as $\hat{x}E_0\cos(\omega_s t + k_s z + \Phi)\exp[-(x^2 + y^2)/W_0^2]$. A dimensionless laser strength parameter a_0 is commonly used to demarcate the linear and nonlinear regimes of the scattering process. In MKS units, a_0 is defined as $(qE_0/m_0c\omega_s)$ or (qA_0/m_0c), where A_0 and E_0 are the respective amplitudes of the vector magnetic potential and the electric field of the laser beam, ω_s is the frequency of operation of the laser beam, and m_0 is the electron rest mass. When the dimensionless laser strength parameter $a_0 \ll 1$, only linear Thomson (linear Compton) scattering is significant. In this limit, it can be shown that the spectral energy radiated per solid angle simplifies to (Esarey *et al.* 1993)

$$\frac{dW(\hat{r},\omega)}{d\Omega} = \frac{q^2\omega^2}{4\pi\varepsilon_0 c}\sum_{f=-\infty}^{\infty}\left[f^2\frac{\omega_d^2}{\omega^2}\left(\frac{1-\cos^2\phi_0\sin^2\theta_0}{\sin^2\theta_0\cos^2\phi_0}\right)\right.$$
$$\left. + \beta_0^2\sin^2\theta_0 - 2f\frac{\omega_d}{\omega}\beta_0\cos\theta_0\right]J_f^2(\Delta)\delta^2(\tilde{\omega} - f\omega_d), \qquad (1)$$

where $\Delta = (-a_0/\gamma_0)(\omega/\omega_d)\sin\theta_0\cos\phi_0\exp[-(x_0^2 + y_0^2)/W_0^2]$, $\omega_d = \omega_s(1 + \beta_0)$, $\beta_0 = v_0/c$, and $\tilde{\omega} = \omega(1 - \beta_0\cos\theta_0)$. The phase terms are omitted because this information is lost in the power calculation. The frequency width of the radiation spectrum is assumed to be sharply peaked about the resonant frequency dictated by the delta function as

$$\omega = \frac{f\omega_d}{(1 - \beta_0\cos\theta_0)}. \qquad (2)$$

The delta function can be equivalently represented as

$$\delta^2(\chi\omega + \psi) = \lim_{T\to\infty}\left\{\left[\frac{1}{4\pi^2}\int_{-T/2}^{T/2}\exp[i(\psi + \chi\omega)t]\,dt\right]\int_{-T/2}^{T/2}\exp[i(\psi + \chi\omega)t]\,dt\right\}, \qquad (3)$$

where $\chi = [1 - \beta_0\cos\theta_0]$ and $\psi = -f\omega_d$. Let T be interpreted as the emission period. The spectral energy is expressed as the spectral power if one introduces a factor of T^{-1} in the limiting operation on the right-hand side of equation (3). The differential spectral energy radiated per differential solid angle given by equation (1) becomes the differential spectral power per differential solid angle when $\delta^2(\tilde{\omega} - f\omega_d)$ is replaced by $(1/2\pi)\delta(\tilde{\omega} - f\omega_d)$.

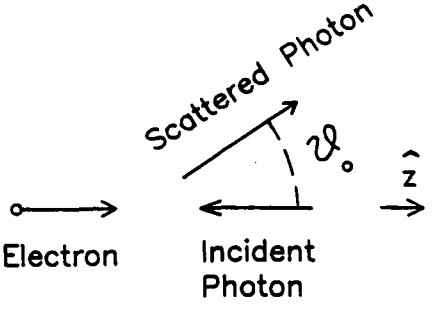

FIGURE 1. The geometrical configuration of the inverse Compton scattering between an electron beam and a laser beam.

The total power expressed in terms of the spectral power is given by $P_T(\hat{r}) = \int_0^\infty P(\hat{r},\omega)d\omega$. Substituting equation (3) into equation (1) directly, the differential power per differential solid angle is

$$\frac{dP_T(\hat{r})}{d\Omega} = \sum_{f=1}^{\infty} \frac{q^2 f^2 \omega_d^2 J_f^2(\Delta)}{8\pi^2 \varepsilon_0 c} \bar{V}(\theta_0, \varphi_0), \tag{4}$$

where

$$\bar{V}(\theta_0,\phi_0) = \frac{1}{[1 - (\beta_0)\cos\theta_0]}\left[\beta_0 \frac{[\beta_0 - \cos\theta_0]}{[1 - \beta_0\cos\theta_0]^2} - \frac{\beta_0\cos\theta_0}{[1 - \beta_0\cos\theta_0]} + \frac{1 - \cos^2\phi_0 \sin^2\theta_0}{\cos^2\phi_0 \sin^2\theta_0}\right]. \tag{5}$$

In the limit as θ approaches zero, only the first harmonic term in the series contributes to the backscattered power per solid angle.

The differential power scattered per solid angle due to a single scatterer is given by equation (4). A pulsed Gaussian electron beam is now considered. The photon–electron collisions generate an incoherent source of light. For the electron and photon (CO_2 and ruby) beams considered, this is reasonable. The wavelength of the CO_2 laser is about 10.6 μm and the beam pulse duration, T_b, is typically on the order of 50 ps. The beam pulse width is approximately $T_b c$ or 15 mm. Because the beam pulse width is large relative to the wavelength of the laser, scattered photons are justifiably incoherent.

Let $N(\mathbf{r}_0)$ be the number of scatterers per unit volume. Then the total differential power scattered per solid angle due to all scatterers in the interaction region is given by multiplying equation (4) by $N(\mathbf{r}_0)$ and integrating over all space. The interaction region is the region of overlap between the two beams. The integration is simplified by representing the Bessel function in terms of its series representation as

$$J_f^2(\Delta) = \sum_{k=0}^{\infty}\sum_{h=0}^{\infty} \frac{(-1)^k(-1)^h \Delta^{2(f+h+k)}}{k!h!\Gamma(f+k+1)\Gamma(f+h+1)}. \tag{6}$$

The pulsed electron beam is assumed to have a Gaussian profile in the plane perpendicular to the direction of free streaming motion. The density of the beam is given by

$$N(\mathbf{r}_0) = N_0 \exp[-(x_0^2 + y_0^2)/W_{eb}^2][U(z_{11}(t) - z_0) - U(z_{12}(t) - z_0)], \tag{7}$$

where N_0 is the electron density on the electron beam axis, W_{eb} is the electron beam waist, $z_{12} - z_{11}$ is the pulse width of the beam, and $U(z)$ is the unit step function. Let L_0 be the length of the overlap between the electron and the laser beams given as

$$L_0 = \frac{v_0 L_p - cL_e}{v + c}.$$

The parameters L_p and L_e are, respectively, the lengths of the photon and the electron beams as measured in the laboratory frame of reference. The total differential power scattered per solid angle due to all electron scatterers is

$$\frac{dP_T(\hat{r})}{d\Omega} = \sum_{f=1}^{\infty}\sum_{h=0}^{\infty}\sum_{k=0}^{\infty} \frac{(-1)^h(-1)^k}{h!k!\Gamma(f+h+1)\Gamma(f+k+1)} \times \frac{q^2 f^2 \omega_d^2 L_0 N_0}{8\pi\varepsilon_0 c} \frac{W_{eb}^2 W_0^2}{2(f+h+k)W_{eb}^2 + W_0^2}\left[\frac{fa_0 \sin\theta_0\cos\phi_0}{2\gamma_0(1 - \beta_0\cos\theta_0)}\right]^{2(f+h+k)} \bar{V}(\theta_0,\phi_0), \tag{8}$$

where the scattered photon frequency is given by equation (2).

Integrating equation (8) over a solid angle, the total power scattered between $\theta_{0_{min}}$ and $\theta_{0_{max}}$ is given by

$$P_T = \sum_{f=1}^{\infty}\sum_{h=0}^{\infty}\sum_{k=0}^{\infty} \frac{(-1)^h(-1)^k}{h!k!\Gamma(f+k+1)\Gamma(f+h+1)} \frac{q^2f^2\omega_a^2L_0N_0}{8\pi\varepsilon_0 c} \times \frac{W_{eb}^2W_0^2}{2(f+h+k)W_{eb}^2+W_0^2}\left[\frac{fa_0}{2\gamma_0}\right]^{2(f+h+k)} [\beta_0^2S_{fhk}^a - \beta_0 S_{fhk}^b + S_{fhk}^c - S_{fhk}^d], \quad (9)$$

where

$$S_{fhk}^a = 2\pi\left[\prod_{b=1}^{f+h+k}\frac{(2b-1)}{2b}\right]\left[\int_{x_{min}}^{x_{max}} \frac{(1-x^2)^{f+h+k}}{(1-\beta_0 x)^{2(f+h+k)+3}}\,dx - \frac{c}{v_0}\int_{x_{min}}^{x_{max}} \frac{x(1-x^2)^{f+h+k}}{(1-\beta_0 x)^{2(f+h+k)+3}}\,dx\right] \quad (10a)$$

$$S_{fhk}^b = 2\pi\left[\prod_{b=1}^{f+h+k}\frac{(2b-1)}{2b}\right]\int_{x_{min}}^{x_{max}} \frac{x(1-x^2)^{f+h+k}}{(1-\beta_0 x)^{2(f+h+k)+2}}\,dx \quad (10b)$$

$$S_{fhk}^c = 2\pi\left[\begin{array}{ll} 1 & \text{for } f=1,\ h=k=0 \\ \prod_{b=1}^{f+h+k-1}\frac{(2b-1)}{2b} & \text{otherwise}\end{array}\right]\int_{x_{min}}^{x_{max}} \frac{(1-x^2)^{f+h+k-1}}{(1-\beta_0 x)^{2(f+h+k)+1}}\,dx \quad (10c)$$

$$S_{fhk}^d = 2\pi\left[\prod_{b=1}^{f+h+k}\frac{(2b-1)}{2b}\right]\int_{x_{min}}^{x_{max}} \frac{(1-x^2)^{f+h+k}}{(1-\beta_0 x)^{2(f+h+k)+1}}\,dx. \quad (10d)$$

The limits of integration are given as

$$x_{max} = \cos\theta_{0_{min}} \quad (11a)$$

$$x_{min} = \cos\theta_{0_{max}}. \quad (11b)$$

It is interesting to note from equation (9) that the optimized scattered powder does not in general occur when the electron beam waist is equal to the waist of the laser beam.

The half-bandwidth resolution on both sides of the center frequency of the scattered radiation ω located at an angle θ_0 from the backscattered direction are

$$\theta_{0_{min}} = \cos^{-1}\left[\frac{\beta\cos\theta_0 + \frac{\Delta\omega}{2\omega}}{\beta\left(1+\frac{\Delta\omega}{2\omega}\right)}\right] \quad (12)$$

$$\theta_{0_{max}} = \cos^{-1}\left[\frac{\beta\cos\theta_0 - \frac{\Delta\omega}{2\omega}}{\beta\left(1-\frac{\Delta\omega}{2\omega}\right)}\right], \quad (13)$$

where

$$\theta_0 = \cos^{-1}\left[\frac{1}{\beta}\left\{1 - f(1+\beta)\left(\frac{\omega_s}{\omega}\right)\right\}\right]. \quad (14)$$

For a laser beam of frequency ω_s, the scattered radiation of center frequency ω and full bandwidth $\Delta\omega$ subtends the angle $\theta_{0_{max}} - \theta_{0_{min}}$ about θ_0. In the special case when the scattered

frequency of radiation is the maximum frequency generated ($\theta_0 = 0$), the full bandwidth radiation subtends the angle $0 < \theta_0 < 2\theta_{0_{max}}$. Once a bandwidth is specified, the angle in which the radiation subtends is fixed.

In equations (8) and (9), the term

$$\frac{W_{eb}^2 W_0^2}{2(f + h + k)W_{eb}^2 + W_0^2} \tag{15}$$

is due to the overlap in cross section between the two beams resulting from their Gaussian nature. As f, h, and k increase in value, equation (15) approaches

$$\frac{W_0^2}{2(f + h + k)}.$$

For small integer values of f, h, and k, the dominant term in the series of equation (9) occurs when $f = 1$ and $h = k = 0$. Consequently, the total power is seen to be nearly linearly related to the laser intensity, the length of interaction, and the electron beam density. Further, equations (8) and (9) can be significantly simplified if h and k are set equal to zero. Using the series definition of the Bessel function, equations (8) and (9), respectively, simplify to

$$\frac{dP_T}{d\Omega} \approx \sum_{f=1}^{\infty} \frac{q^2 f^2 \omega_d^2 L_0 N_0}{8\pi\varepsilon_0 c} \frac{W_{eb}^2 W_0^2}{2fW_{eb}^2 + W_0^2} J_f^2\left(\frac{fa_0}{\gamma_0} \frac{\sin\theta_0 \cos\phi_0}{(1 - \beta_0 \cos\theta_0)}\right) \tilde{V}(\theta_0, \phi_0) \tag{16}$$

$$P_T \approx \sum_{f=1}^{\infty} \frac{q^2 f^2 \omega_d^2 L_0 N_0}{8\pi\varepsilon_0 c} \frac{W_{eb}^2 W_0^2}{2fW_{eb}^2 + W_0^2} J_f^2\left(\frac{fa_0}{\gamma_0}\right)[\beta_0^2 S_{f00}^a - \beta_0 S_{f00}^b + S_{f00}^c - S_{f00}^d]. \tag{17}$$

Equations (16) and (17) are useful when examining large values of f in the series. Equations (8) and (9) appear to indicate for large enough f that successive terms in the series increase, yielding a divergent series. With the aid of the large order asymptotic expansion of the Bessel function,

$$J_n(x) \approx \frac{1}{\sqrt{2\pi n}}\left(\frac{ex}{2n}\right)^n.$$

Equations (16) and (17) demonstrate that the series only diverges when $a_0 > 0.736\gamma_0$. In this case, a nonlinear theory is required to correctly characterize the scattered radiation.

3. Verification and validity

In quantum mechanics, it is customary to define the probability of an event by means of cross sections. The Thomson differential cross section characterizes the probability that an electron and a photon will collide when (Tucker 1975; Longair 1992) $\gamma\hbar\omega_s \ll m_e c^2$. Here, m_e is the rest mass of the electron and $\hbar\omega_s$ is the incident source photon energy in the laboratory frame of reference. The Thomson cross section is derived from classical theory. An electron moving with relativistic velocities can exist in four states instead of two. This is a consequence of the two spin directions an electron can possess (Tucker 1975; Longair 1992). Classical theory cannot account for these states. As a result, one must use the Klein–Nishina formula for the differential cross section when $\gamma\hbar\omega_s \geq m_e c^2$.

The maximum electron energies of interest are on the order of 50 MeV. Both the ruby (1.79 eV) and the CO_2 (0.117 eV) lasers are typical light sources. The relativistic factor for a 50-MeV electron is approximately 97.8. The rest mass of the electron is $m_e = 0.511$ MeV. The classical approximation is well suited under these conditions. Therefore, scattering from typical electron beam energies between 10 and 35 MeV is well within the classical approximation.

Conservation of energy and momentum considerations dictate that the scattered photon frequency, ω, is given by (Longair 1992)

$$\omega = \frac{\left(1 - \frac{v_0}{c}\cos\theta\right)\omega_s}{\left(1 - \frac{v_0}{c}\cos\theta_0\right) + \frac{\hbar\omega_s}{\gamma m_e c^2}(1 - \cos\alpha)}, \tag{18}$$

where θ is the angle between the incoming photon and the velocity vector of the electron, θ_0 is the angle between the scatted photon and electron after interaction, α is the scattering angle (angle between the incident and scattered photons), m_e is the electron rest mass, and $\hbar$ is 2π times the Planck's constant. In equation (18), $\theta = 180°$ for head-on collisions. For electron energies between 1 and 50 MeV and photon energies on the order of 0.117 and 1.79 eV,

$$\frac{\hbar\omega_s}{\gamma m_e c^2}(1 - \cos\alpha) \ll \left(1 - \frac{v_0}{c}\cos\theta_0\right)$$

for all values of α and θ_0. Consequently, equation (18) simplifies in this limit to the scattered frequency predicted from classical theory for head-on collisions [see equation (2)]. For a 50-MeV electron colliding head-on with a ruby photon, the classical scattered frequency obtained from equation (2) yields a 0.14% worst-case error compared to that obtained from equation (18). Decreasing the energy decreases the worst-case error.

Consider the limit when the initial beam energy approaches zero. The light wave with $\hat{x}$-directed polarization causes an oscillatory current directed in the $\hat{x}$-direction. The radiation pattern of this current should be similar to that of the Hertzian dipole. The radiation intensity of a Hertzian dipole positioned along the $\tilde{z}$-axis in a spherical coordinate system is proportional to $\sin^2\tilde{\theta}$, where $\tilde{\theta}$ is the angle of declination measured positively from the $\tilde{z}$-axis. The radiation intensity is independent of the azimuthal angle. In the limit when $v_0 \to 0$ with $f = 1$ and $h = k = 0$, the angular dependence of the total differential power scattered per differential solid angle as seen from equations (8) and (5) is

$$\frac{dP_T}{d\Omega} \propto [1 - \cos^2\phi_0 \sin^2\theta_0].$$

Consider the rotated coordinate system with the $\tilde{z}$-axis along the x-axis and the $\tilde{y}$-axis along the y-axis. Transforming between spherical coordinates in the two systems $[(r_0, \theta_0, \phi_0)$ and $(\tilde{r}, \tilde{\theta}, \tilde{\phi})]$, it can be shown that $\cos^2\phi_0 \sin^2\theta_0 = \cos^2\tilde{\theta}$. Consequently,

$$\frac{dP_T}{d\Omega} \propto \sin^2\tilde{\theta}.$$

The angular distribution of the differential power for these two sources is equivalent, as expected.

Assume that a 20-MeV, 3-nC electron beam with a 10-mm waist collides head-on with a 2-J CO_2 (0.117-eV) laser beam with a 10-mm waist. The photon beam and the electron beam pulse durations are, respectively, 5 ns and 500 ps. Table 1 illustrates that higher order harmonics negligibly contribute to the overall power. Further, the dominate term in the Bessel series is the $h = k = 0$ term. Higher order terms do not significantly affect the total power calculation in the accuracy presented. Consequently, forcing $f = 1$ and $h = k = 0$, it can be shown with the aid of integral tables (Prudnikov *et al.* 1986) that $\beta_0^2 S_{fhk}^a - \beta_0 S_{fhk}^b + S_{fhk}^c - S_{fhk}^d = (\frac{8}{3})\pi\gamma_0^4$. Equation (9) simplifies to

$$P_T = \frac{8\pi}{3} r_e^2 L_0 N_0 (1 + \beta)^2 \gamma_0^2 P_0, \tag{19}$$

TABLE 1. Total power for various harmonic numbers (f) valid for $h_{max} = k_{max} = 0$, 1, and 4

Harmonic Number f	CO_2 Laser (mW)	Ruby Laser (W)
1	46.22	52.975
2	2.935×10^{-7}	1.996×10^{-8}
3	3.386×10^{-15}	1.366×10^{-17}

The total power appears to be insensitive to the truncation of the h and k series of equation (9) characterizing the Bessel functions in equation (6). Note, $h = 0$ to h_{max} and $k = 0$ to k_{max} in the series. It is observed that those harmonic terms in the power series [see equation (9)] with $f > 1$ contribute negligibly to the total scattered power.

where $r_e = q^2/(4\pi\varepsilon_0 m_0 c^2)$ and $P_0 = (|E_0|^2/2\eta_0)\pi[(W_{eb}^2 W_0^2)/(2W_{eb}^2 + W_0^2)]$. Here, r_e is the classical electron radius in the MKS system, η_0 is the intrinsic impedance of free space, and P_0 is the time average power in the region of overlap between the Gaussian laser beam and the Gaussian electron beam. Equation (19) is identical with the power obtained from the relativistic Larmor formula (Esarey *et al.* 1993).

4. Application and discussion

A particular linear accelerator is capable of generating about 10 nC of 35-MeV electrons at best. Optimal operation is within the 10- to 20-MeV range. Typically, 2-J CO_2 and 10-J ruby-pulsed lasers are accessible. The power scattered upon the electron–photon beam interaction is examined.

Consider that a 20-MeV, 3-nC electron beam with a 10-mm waist collides head-on with a 2-J CO_2 (0.117-eV) laser beam with a 10-mm waist. The photon beam and the electron beam pulse durations are, respectively, 5 ns and 500 ps. As shown in figure 2, a 712-eV backscattered photon ($\theta_0 = 0$) is generated. Figure 3 indicates how the power is distributed in increments of ($\Delta\theta_0 =$) 0.2°. About 88, 61, and 27% of the total scattered power (46.22 mW) are contained in 2, 1, and 0.5° conical cones, respectively. Note that the power *density* is highest in the first increment, $0° \leq \theta \leq 0.2°$, and decreases monotonically in successive increments. As seen in figure 2, the respective energy bandwidths are 460, 220, and 77 eV.

Now suppose that a 30-MeV, 10-nC electron beam with a 6-mm waist collides head-on with a 10-J ruby (1.79-eV) laser beam with a 6-mm waist. The photon beam and electron beam pulse durations are, respectively, 5 ns and 50 ps. At $\hat{x}E_0\cos(\omega_s t + k_s z + \Phi)\exp[-(x^2 + y^2)/W_0^2]$, the backscattered photon energy is 24.5 keV, as seen in figure 4. The distribution of the power in 0.2° increments is displayed in figure 5. About 96, 79, and 46% of the total scattered (52.975 W) power are contained in 2, 1, and 0.5° conical cones, respectively. As seen in figure 4, the respective energy bandwidths are about 20, 12.1, and 5 keV. Sensitive windowless X-ray detectors are capable of measuring powers of this magnitude.

As long as the laser beam energy is the same, the total scattered power is independent of the photon (laser) source used. That is, if a 10-J CO_2 laser is used in place of a 10-J ruby source having the same pulse configuration, then the total power is given by figure 4. This is reasonable because the number of CO_2 photons in a 10-J pulse is much larger than the number of ruby photons even though the energy of each CO_2 photon is smaller than the ruby photon. Therefore, a 10-J CO_2 laser will generate about 24.4 W of power within a 0.5° conical cone having an energy bandwidth of 77 eV.

A self-consistent power relation for linear inverse Compton scattering has been developed and compared to classical dipole radiation and radiation from a moving electron beam as obtained from a Larmor formulation. Power coupling among the fundamental and harmonic

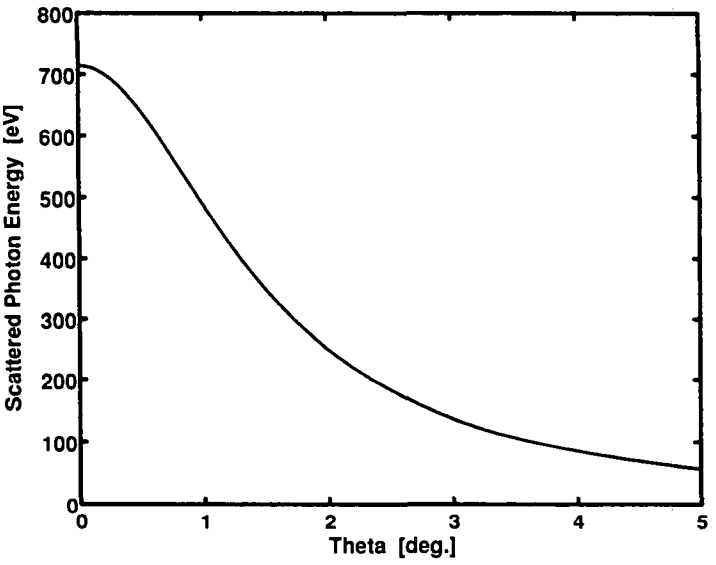

FIGURE 2. The scattered photon energy as a function of the angle of declination from the initial electron beam velocity. A Gaussian profile, focused, 2-J pulsed, CO_2 laser beam collides head-on with a Gaussian profile, 20-MeV, 3-nC, pulsed electron beam. Both beams have a 10-mm beam waist. The electron and photon pulse durations are, respectively, 500 ps and 5 ns.

modes is demonstrated, but appears negligible for the electron beam and laser beam parameters of interest. It is demonstrated that pulse mode calibration of sensitive X-ray detectors is possible when inverse Compton-scattered radiation between a medium energy electron beam driven by a linear accelerator collides with an infrared (CO_2) or red light (ruby) laser beam.

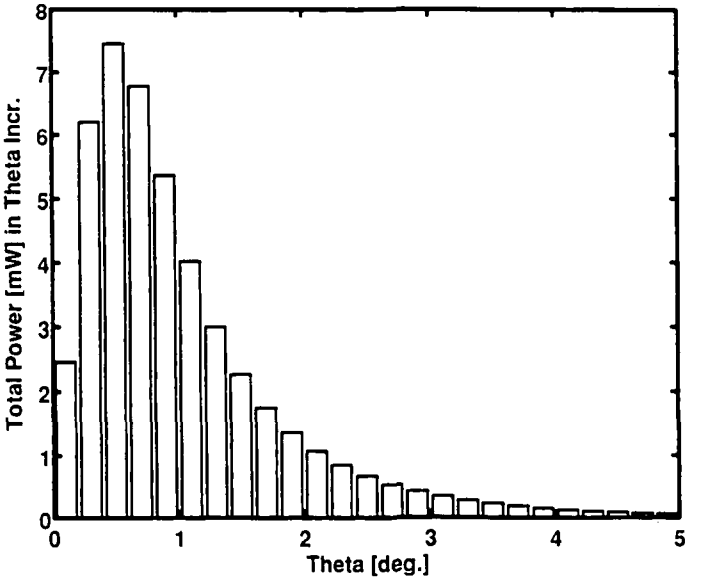

FIGURE 3. The total power in angular bins of $\Delta\theta = 0.2°$ for the head-on collision between the CO_2 laser beam and the electron beam of figure 2.

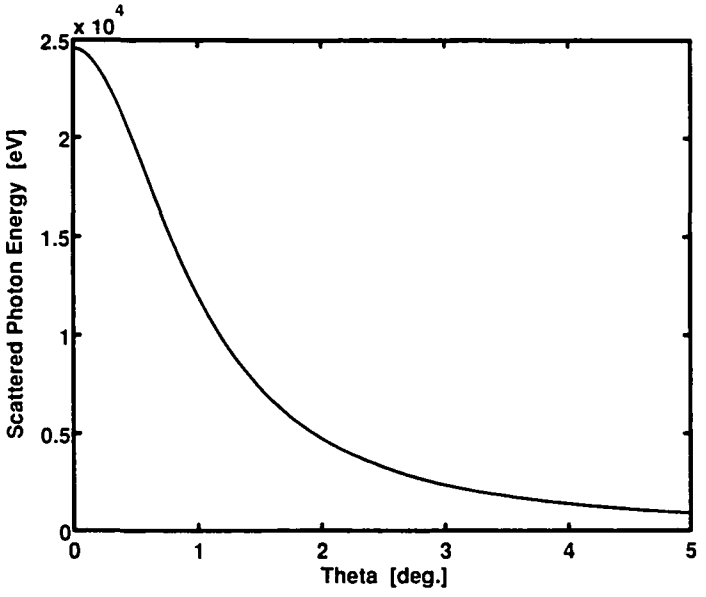

FIGURE 4. The scattered photon energy as a function of the angle of declination from the initial electron beam velocity. A Gaussian profile, focused, 10-J pulsed, ruby laser beam collides head-on with a Gaussian profile, 30-MeV, 10-nC, pulsed electron beam. Both beams have a waist of 6 mm. The electron and photon pulse durations are, respectively, 50 ps and 5 ns. Compared to figure 2, the maximum scattered photon energy is about three times larger. Further, the scattered photon energy is more sensitive to the angular position of the observer.

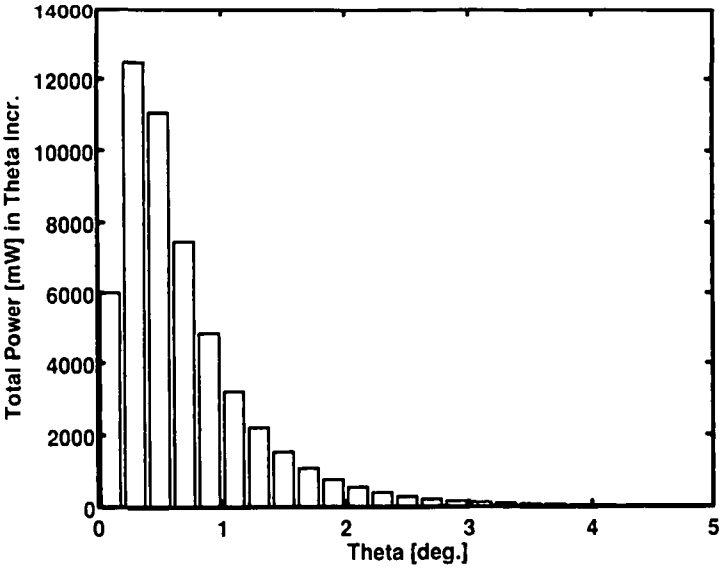

FIGURE 5. The total power in angular bins of $\Delta\theta = 0.2°$ for the head-on collision between the ruby laser beam and the electron beam of figure 4. Sensitive detectors are capable of measuring powers of this magnitude.

REFERENCES

BARDSLEY, J.N. *et al.* 1989 *Phys. Rev. A* **40**, 3823.

BROWN, L.S. & KIBBLE, T.W.B. 1964 *Phys. Rev.* **133**, A705.

ESAREY, E. *et al.* 1993 *Phys. Rev. E* **48**, 3003.

JACKSON, J.D. 1975 *Classical Electrodynamics*, 2nd ed. (John Wiley, New York).

KIM, K.J. 1989 *AIP Conf. Proc. I*, 565.

LONGAIR, M.S. 1992 *High Energy Astrophysics, Vol. 1, Particles, Photons and their Detection*, 2nd ed. (Cambridge University Press, New York).

MOHIDEEN, U. *et al.* 1992 *J. Opt. Soc. Am. B* **9**, 2190.

PRUDNIKOV, A.P. *et al.* 1986 *Integrals and Series, Vol. 1.* (Gordon and Breach Science Publ., New York).

RIDE, S. *et al.* 1995 *Phys. Rev. E* **52**, 5425.

ROBERSON, C.W. & SPRANGLE, P. 1989 *Phys. Fluids B* **1**, 3.

SARACHIK, E.S. & SCHAPPERT, G.T. 1970 *Phys. Rev. D* **1**, 2738.

SCHILL JR., R.A. & MCCREA, E. 1997 *Laser Part. Beams* **15**, 179.

SPRANGLE, P. & ESAREY, E. 1992 *Phys. Fluids B* **4**, 2241.

SPRANGLE, P. *et al.* 1989 *Appl. Phys. Lett.* **55**, 2559.

SPRANGLE, P. *et al.* 1992 *J. Appl. Phys.* **72**, 5032.

TRAN, T.M. *et al.* 1987 *IEEE J. Quant. Electron.* **QE-23**, 1578.

TUCKER, W.H. 1975 *Radiation Processes in Astrophysics.* (MIT Press, Cambridge).

VACHASPATI 1962 *Phys. Rev.* **128**, 664.